Scientific Research Publishing

Open Journal of Geology, 2017, 7, 1465-1477
http://www.scirp.org/journal/ojg
ISSN Online: 2161-7589
ISSN Print: 2161-7570

Mineral Chemistry of Wehrlite Xenoliths Hosted in Basalts from the SW of Hosséré Dammougalré (Adamawa Plateau, Cameroon): Thermobarometric Implications

Isaac Bertrand Gbambié Mbowou[1*], Dagwaï Nguihdama[2], Fadimatou Ngounouno Yamgouot[3], Mama Ntoumbe[1], Abdel Aziz Youpoungam[1], Ismaïla Ngounouno[1]

[1]School of Geology and Mining Engineering, University of Ngaoundere, Ngaoundere, Cameroon
[2]Department of Life and Earth Sciences, Higher Teachers' Training College, University of Maroua, Maroua, Cameroun
[3]Department of Earth Sciences, Faculty of Science, University of Ngaoundere, Ngaoundere, Cameroon
Email: *mbowou2000@yahoo.fr

How to cite this paper: Mbowou, I.B.G., Nguihdama, D., Yamgouot, F.N., Ntoumbe, M., Youpoungam, A.A. and Ngounouno, I. (2017) Mineral Chemistry of Wehrlite Xenoliths Hosted in Basalts from the SW of Hosséré Dammougalré (Adamawa Plateau, Cameroon): Thermobarometric Implications. *Open Journal of Geology*, **7**, 1465-1477.
https://doi.org/10.4236/ojg.2017.710098

Received: August 24, 2017
Accepted: October 13, 2017
Published: October 16, 2017

Abstract

Wehrlite samples (size: ~4 cm) hosted in basaltic lavas from the SW of Hosséré Dammougalré are located in the western Adamawa Plateau. Porphyritic and allotriomorphic texture characterize respectively host Basalt and wehrlite xenoliths. The phenocrysts of olivine (Fo_{68-74}), and Ti-magnetite are scattered in host basalt. Wehrlite xenoliths (~4 cm size) contain Cr-rich clinopyroxene (diopise-augite), olivine (Fo_{76-88}) and chromiferous spinel. Equilibrium temperatures calculated from Fe/Mg exchange reaction for olivine/spinel vary between 944˚C and 1102˚C. The wehrlite olivine crystals with low Fo (<90) indicate a re-equilibration of Fe-Mg in the host basalt at low temperatures. All the analyzed wehrlite clinopyroxenes have crystallized at high pressures as evidenced by the Al^{vi} and Al^{iv} contents. The studied spinel-bearing wehrlite xenoliths represent probably the residual portions of the upper mantle, which are an important source of information about lithospheric composition and thermal evolution beneath the Adamawa Plateau.

Keywords

Wehrlite, Adamawa Plateau, Hosséré Dammougalré, Mineral Chemistry, Geothermometry

1. Introduction

The accidental fragments called rock xenoliths, piked up by the turbulent host

magma on its ascent, allowed to characterize petrologically the Earth's upper mantle. They are an important source of information about lithospheric composition and thermal evolution in mantle regions associated with alkaline volcanism [1]. In the Adamawa Plateau (**Figure 1**), previously ultramafic xenoliths data are from Dibi area ([2] [3]), Youkou maar [4], Ngao Voglar [5] and Hosséré Garba [6]. These ultramafic xenoliths studied are chiefly of dunite and lherzolite composition. Thus, the discovery of the wehrlite samples from the SW of Hosséré Dammougalré could improve the knowledge of the upper mantle beneath the Adamawa Plateau. Indeed, wehrlite samples hosted in basaltic lavas from the SW of Hosséré Dammougalré are located in the western Adamawa Plateau (**Figure 1**). Adamawa Plateau is a tectonomagmatic domain bordered by faults oriented N70˚E [7]. This plateau presented as the horst, is situated to the north of the Congo Craton, as the result of the fold belt shearing, oriented WSW-ENE [8].

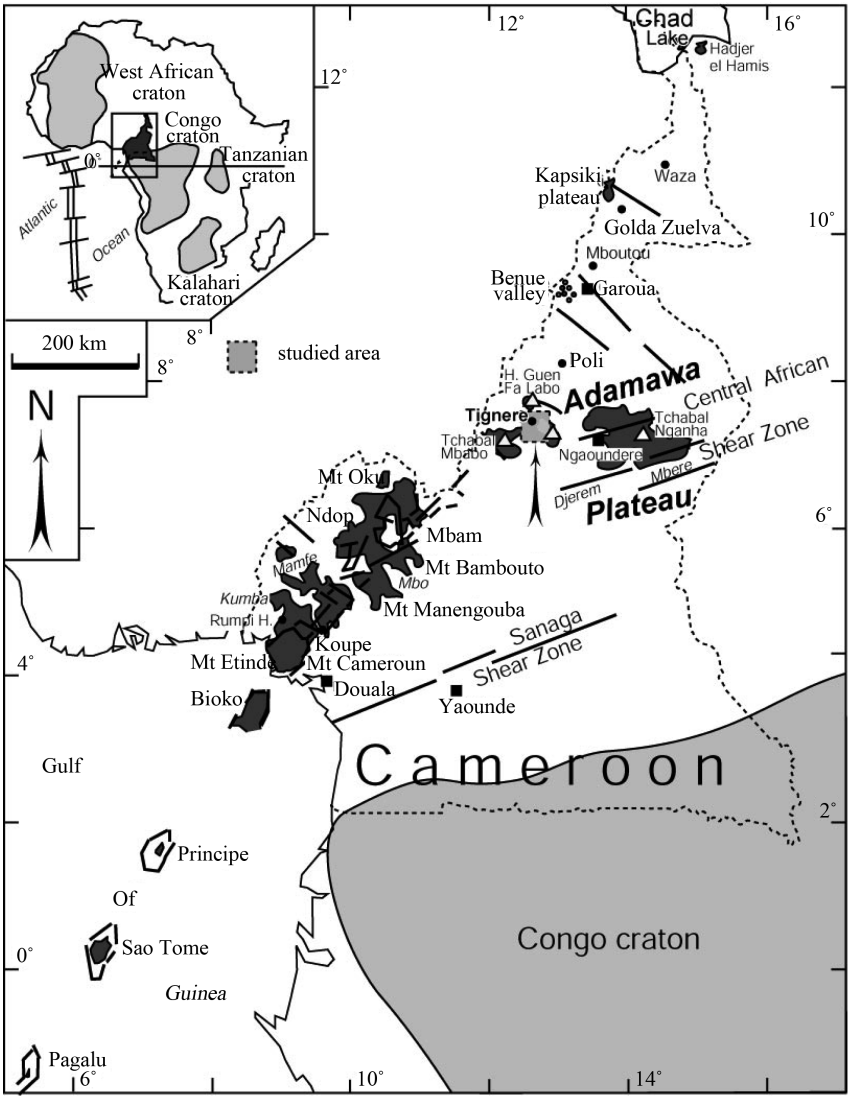

Figure 1. Location of the studied zone in the Adamawa Plateau domain.

The aims of this paper are to present the first petrographical, mineral chemistry and thermobarometric data of the wehrlite xenoliths from the SW of Hosséré Dammougalre, chiefly to enhance the knowledge of upper mantle beneath the Adamawa Plateau.

2. Geological Description of the Studied Zone

The geological sketch established for the studied zone is presented (**Figure 2**). The trachytic outcrops of Hosséré Dammougalré and Hosséré Doro are surrounded by several basaltic units (lower, middle and upper). *The lower basaltic units* were almost completely weathered and converted into black reddish ferralitic soils or the clusters of residual ferruginous vacuolar cuirasses. *The intermediate or middle basaltic units* were fragmented into angular or rounded blocks of various sizes (5 - 50 cm), slightly weathered and dispersed. *The upper basaltic units* were represented by the blocks accumulated as small isolated hills (diameter: ~500 m; height <30 m). These hills consist of small prismatic blocks (0.2 - 1.7 m) and vertical columnar jointing (0.5 to 2 m) of basalt. The studied xenoliths (size: ~4 cm) were sampled within these upper basaltic units at the SW of Hosséré Dammougalré. The Hosséré Dammougalré (altitude: ~1600 m a.s.l) is a neck of needle-shaped lava which have circular basis (diameter: ≈200 m) and more or less steep slopes (45˚ - 90˚). This formation is strongly prismatic and dismantled into blocks, disseminated in chaos on the soil. However, the Hosséré Doro is a dome bounded by small steep cliffs (20 - 40 m high) and the lava blocks are accumulated to the foothill.

3. Analytical Methods

The mineral phases were analyzed in polished thin sections with the electron microprobe analyzer using a Cameca microprobe SX100 at the "Université Pierre et Marie Curie", Paris VI (France). The standards data used for analysis are from natural (Si, Al and K on orthoclase, Ca on anorthite, Na on albite, P on apatite, Zr on zircon) and synthetic (Fe on Fe_2O_3, Ba on BaO_4, Sr on $SrSiO_3$)

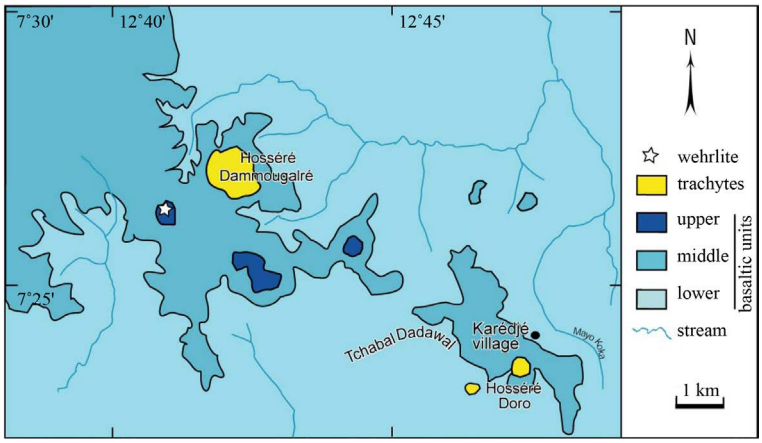

Figure 2. Sketch of the geological map of the studied zone.

phases.

The measurements were carried out with a beam size of 10 - 100 μm, under the following conditions expressed in kV (accelerating voltage), nA (beam current) and s (counting times at the peak): Olivine (15 kV, 40 nA, 20 s for all elements, except Si (10 s)), clinopyroxene (15 kV, 40 nA, 20 s for Si, Al, Fe, Mg, Ca, Na, Mn and 30 s for Ti and Zr), feldspar (15 kV, 10 nA, 5 s for all elements), Fe-Ti oxides and spinel (15 kV, 40 nA, 40 s for Ti, Fe, Mn, Mg, 10 s for Si, 15 s for Cr and 30 s for Al). Measurements correction was carried out using the "PAP" program [9].

4. Results

4.1. Petrography

Host Basalt is characterized by a porphyritic texture. The phenocrysts of olivine (~2 mm), clinopyroxene (1.2 - 2.1 mm) and Fe-Ti oxides (0.5 - 0.6 mm) are scattered in a groundmass consisting of clinopyroxene, Fe-Ti oxides and plagioclase microlites. Olivine phenocrysts are subhedral, cracked and their edges are sometimes destabilized into iddingsite. Clinopyroxene phenocrysts are euhedral and twinned.

Wehrlite xenoliths (~4 cm size) are characterized by an allotriomorphic texture, with inequigranular olivine (~40 vol.%), clinopyroxene (~55 vol.%) and spinel (~5 vol.%) crystals. Spinel crystals are red brown and interstitial between the crystals of olivine and clinopyroxene. The contact between the host basalt and wehrlite xenoliths is materialized by the accumulation of small Fe-Ti oxides and plagioclase crystals or the tiny host basalt veins.

4.2. Mineral Chemistry

4.2.1. Olivine

In the host basalt, forsterite (Fo) values calculated for the analyzed olivine phenocrysts (**Table 1**) reach 73 - 74 and 68 - 72, respectively for the core and the rim. The CaO contents are high (rim, up to 0.43 wt% and core, up to 0.41 wt%). Using bulk-rock composition as a liquid at the total pressure of 1 atm, the crystallization temperatures were estimated after [10] for the core and the rim respectively to 1224˚C ± 60˚C and 1166˚C ± 48˚C.

For wehrlite xenoliths, the forsterite component (**Table 1**) range from 76 to 88. These values are similar to those calculated for the wehrlites from the Mount Cameroun ($Fo_{82\text{-}86}$; [11]). NiO contents reaching 0.19 wt% and CaO up to 0.39 wt%.

4.2.2. Clinopyroxene

The clinopyroxene phenocrysts (**Table 2**) of the host basalt are both diopside and augite (after the nomenclature of [12]; **Figure 3**). Their Cr_2O_3 contents range from 0 wt% to 0.38 wt%), while TiO_2 and Al_2O_3 contents are high (up to 3.9 wt% and 8.7 wt% respectively). The high contents of Ti and Al^{iv} (apfu: atom

per formula unit) in diopside and augite are linked to a low-pressure of crystallization [13].

Wehrlites contain also diopside and augite, but poor in Al_2O_3 (1.8 - 5.1 wt%), TiO_2 (0.8 - 1.7 wt%) and rich in Cr_2O_3 (up to 0.59 wt%) with Cr# (= 100 × atomic Cr/(Cr+Al)) up to 15.6.

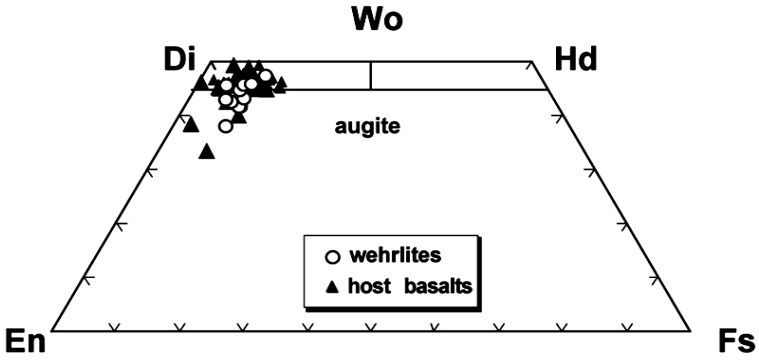

Figure 3. Wo-En-Fs ternary diagram (after Morimoto, 1989) for the classification of clinopyroxene from the studied rocks.

Table 1. Representative compositions of olivine of the host basalt and the studied wehrlite.

rocks	host basalt						wehrlite							
sample nb.	132	132	132	132	132	132	132-1	132-1	132-1	132-1	132-1	132-1	132-1	132-1
description	ph,r	ph,c	ph,c	ph,c	ph,c	ph,r								
SiO_2 (wt%)	37.02	37.09	37.07	37.15	36.62	37.98	38.27	37.43	38.39	38.99	38.86	37.31	36.36	36.74
Al_2O_3	0.10	0.06	0.00	0.00	0.11	0.04	0.01	0.02	0.00	0.07	0.09	0.05	0.00	0.00
FeO	27.25	24.15	24.50	23.99	24.69	25.29	18.58	19.22	19.46	15.09	15.71	15.95	22.86	23.62
MnO	0.92	0.58	0.60	0.60	0.40	0.57	0.37	0.20	0.42	0.05	0.17	0.21	0.53	0.51
MgO	32.93	36.18	36.33	36.51	36.52	35.87	41.84	41.33	41.78	44.54	44.73	44.81	37.83	37.30
CaO	0.30	0.41	0.39	0.38	0.36	0.43	0.30	0.29	0.32	0.15	0.17	0.15	0.36	0.39
NiO	0.09	0.16	0.12	0.09	0.04	0.11	0.04	0.05	0.15	0.17	0.11	0.19	0.00	0.08
Total	98.73	98.64	99.00	98.73	98.74	100.28	99.41	98.55	100.50	99.05	99.83	98.67	97.93	98.64
Si (apfu)	1.008	0.990	0.987	0.990	0.976	1.002	0.982	0.971	0.978	0.988	0.978	0.949	0.968	0.975
Al	0.003	0.002	0.000	0.000	0.003	0.001	0.000	0.001	0.000	0.002	0.003	0.001	0.000	0.000
Fe^{2+}	0.620	0.522	0.518	0.513	0.505	0.558	0.364	0.359	0.371	0.297	0.289	0.237	0.444	0.475
Mn	0.021	0.013	0.013	0.014	0.009	0.013	0.008	0.004	0.009	0.001	0.004	0.004	0.012	0.011
Mg	1.337	1.440	1.441	1.450	1.451	1.411	1.601	1.598	1.587	1.682	1.678	1.699	1.501	1.476
Ca	0.009	0.012	0.011	0.011	0.010	0.012	0.008	0.008	0.009	0.004	0.005	0.004	0.010	0.011
Ni	0.002	0.003	0.002	0.002	0.001	0.002	0.001	0.001	0.003	0.003	0.002	0.004	0.000	0.002
Fo (%)	68	73	74	74	74	72	81	82	81	85	85	88	77	76
Fa	32	27	26	26	26	28	19	18	19	15	15	12	23	24
mg#	68.30	73.41	73.56	73.84	74.17	71.66	81.49	81.65	81.07	84.99	85.29	87.74	77.16	75.65

ph.r: phenocryst. rim; ph.c: phenocryst core.

Table 2. Representative compositions of clinopyroxene of the host basalt and the studied wehrlite.

rocks	host basalt				wehrlite														
sample nb.	132	132	132	132	132-1	132-1	132-1	132-1	132-1	132-1	132-1	132-1	132-1	132-1	132-1	132-1	132-1	132-1	132-1
description	ph.c	ph.r	ph.c	ph.c															
SiO_2 (wt%)	44.07	47.59	50.66	47.01	51.06	51.80	51.60	50.69	50.90	51.93	50.99	53.18	51.14	50.43	52.17	50.29	47.72	50.86	51.10
TiO_2	3.91	1.98	0.65	1.95	0.89	1.78	0.97	1.03	0.99	0.93	0.94	1.19	1.21	0.92	0.83	1.16	3.04	1.61	0.93
Al_2O_3	8.75	7.23	5.27	8.29	4.60	4.33	3.20	4.97	4.65	4.87	4.76	1.85	3.86	5.19	4.76	3.73	5.30	3.20	4.70
Cr_2O_3	0.00	0.06	0.25	0.38	0.34	0.55	0.46	0.43	0.37	0.50	0.30	0.51	0.53	0.59	0.43	0.51	0.00	0.49	0.47
FeO	6.92	6.68	6.90	6.21	5.46	4.91	4.53	5.73	5.13	4.91	5.23	4.46	5.24	5.07	5.04	5.85	7.30	5.27	5.46
MnO	0.32	0.21	0.15	0.17	0.13	0.13	0.11	0.12	0.11	0.04	0.02	0.11	0.23	0.16	0.04	0.05	0.00	0.25	0.08
MgO	11.56	13.18	17.67	13.84	15.52	15.00	15.89	16.36	15.31	15.12	15.54	16.27	15.50	15.29	15.35	14.64	12.68	14.86	15.00
CaO	22.34	21.49	17.18	21.21	21.17	20.77	22.17	18.42	20.55	20.66	20.52	21.53	20.93	20.65	20.01	21.97	22.38	22.01	21.05
Na_2O	0.49	0.60	0.68	0.56	0.79	0.59	0.62	0.82	0.89	0.85	0.81	0.71	0.70	0.84	0.72	0.57	0.62	0.47	0.77
Total	98.37	99.02	99.40	99.60	99.94	99.85	99.55	98.57	98.91	99.80	99.12	99.81	99.33	99.12	99.35	98.75	99.04	99.01	99.57
Fe_2O_3 (calc.)	2.91	0.79	2.84	3.14	0.97	0.00	1.84	0.97	1.40	0.00	1.28	0.00	1.01	1.88	0.00	1.77	1.81	0.13	0.00
FeO (calc.)	4.31	5.97	4.35	3.38	4.59	4.91	2.88	4.86	3.88	4.91	4.07	4.46	4.33	3.38	5.04	4.26	5.67	5.15	5.46
Total (calc.)	98.66	99.10	99.69	99.91	100.04	99.88	99.76	98.67	99.05	99.87	99.26	99.81	99.45	99.35	99.40	98.93	99.22	99.06	99.57
Si (apfu)	1.670	1.793	1.850	1.736	1.885	1.907	1.894	1.873	1.879	1.901	1.877	1.948	1.886	1.857	1.919	1.874	1.793	1.892	1.900
Ti	0.111	0.056	0.018	0.054	0.025	0.049	0.027	0.029	0.027	0.026	0.026	0.033	0.033	0.025	0.023	0.032	0.086	0.045	0.026
Al^{VI}	0.061	0.114	0.077	0.097	0.085	0.094	0.032	0.089	0.081	0.111	0.084	0.028	0.053	0.082	0.125	0.038	0.028	0.033	0.105
Al^{IV}	0.330	0.207	0.150	0.264	0.115	0.093	0.106	0.127	0.121	0.099	0.123	0.052	0.114	0.143	0.081	0.126	0.207	0.108	0.100
Cr	0.000	0.002	0.007	0.011	0.010	0.016	0.013	0.013	0.011	0.014	0.009	0.015	0.015	0.017	0.012	0.015	0.000	0.014	0.011
$Fe^{3+\,(VI)}$	0.083	0.022	0.078	0.087	0.027	0.000	0.051	0.027	0.039	0.000	0.035	0.000	0.028	0.052	0.000	0.050	0.051	0.004	0.000
Fe^{2+}	0.136	0.188	0.133	0.104	0.142	0.151	0.088	0.150	0.120	0.150	0.125	0.136	0.134	0.104	0.155	0.133	0.178	0.160	0.170
Mn	0.010	0.007	0.005	0.005	0.004	0.004	0.004	0.004	0.004	0.001	0.001	0.004	0.007	0.005	0.001	0.002	0.000	0.008	0.003
Mg	0.653	0.740	0.962	0.762	0.854	0.823	0.870	0.901	0.842	0.825	0.853	0.888	0.852	0.839	0.842	0.813	0.711	0.824	0.831
Ca	0.907	0.827	0.672	0.839	0.798	0.819	0.871	0.729	0.813	0.810	0.809	0.845	0.827	0.815	0.789	0.877	0.901	0.877	0.799
Na	0.036	0.044	0.048	0.040	0.056	0.042	0.044	0.059	0.064	0.060	0.058	0.050	0.050	0.060	0.051	0.041	0.045	0.034	0.055
Wo (%)	46.56	41.93	33.15	42.43	41.56	43.24	45.41	37.60	42.82	42.95	42.26	44.65	43.11	42.63	41.59	45.54	46.80	45.28	41.86
En	44.87	46.30	59.15	51.33	50.13	47.95	49.65	53.49	50.07	48.27	50.34	47.98	49.18	51.05	49.33	46.93	42.61	45.80	48.29
Fs	8.57	11.77	7.70	6.23	8.31	8.80	4.94	8.91	7.11	8.78	7.40	7.37	7.71	6.32	9.08	7.53	10.59	8.91	9.85
Ti/Al	0.28	0.17	0.08	0.15	0.12	0.26	0.19	0.13	0.14	0.12	0.13	0.41	0.20	0.11	0.11	0.20	0.37	0.32	0.13
Cr*100/(Cr+Al)	0.00	0.56	3.06	2.99	4.70	7.87	8.71	5.53	5.12	6.42	4.09	15.55	8.37	7.07	5.68	8.36	0.00	9.30	5.06

According to the Al^{vi} vs Al^{iv} diagram (**Figure 4**), these clinopyroxene crystals crystalized at high pressure near of the RMC (Refractory Mantle Clinopyroxene, [14]) field.

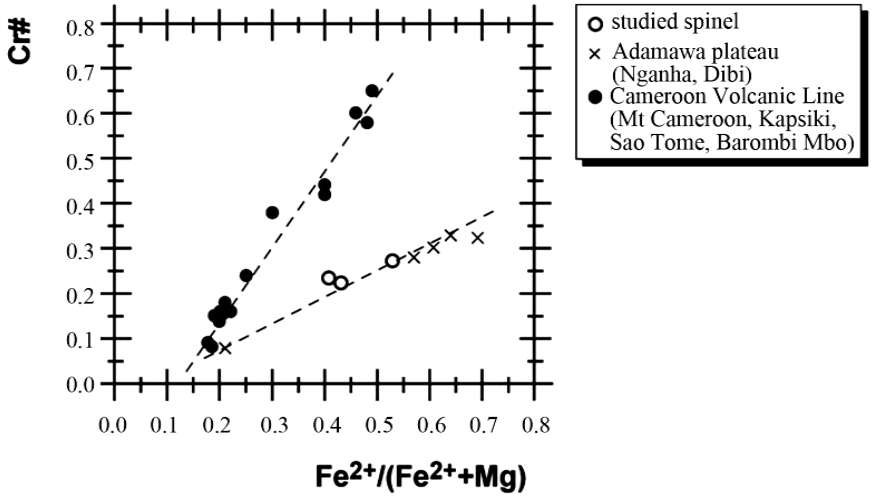

Figure 4. Plot of Cr# vs. $Fe^{2+}/(Fe^{2+} + Mg)$ values of the spinel for xenoliths from the SW of the Hosséré Dammougalré and those of the others sector of the Adamawa Plateau and the Cameroon Volcanic Line.

4.2.3. Fe-Ti Oxides

The titano-magnetite is present in the host basalt (**Table 3**), with TiO_2 and FeO contents reaching respectively 25.0 wt% and 69.5 wt%.

4.2.4. Spinel

Spinel of wherlites (Al > Cr, Mg > Fe^{2+}) is chromiferous with the values of Cr# (Cr × 100/(Cr + Al) and $Fe^{2+}/(Fe^{2+}$ + Mg) positively correlated (**Table 4**; Figure 4). The correlation trend displays on the **Figure 4**, present two distinct evolutions, one for the Adamawa Plateau (Nganha; [15], Dibi; [3]) and another for the Cameroon Volcanic Line (São Tomé; [16], Mbarombi Mbo; [17]), Mount Cameroon; [11] [18] and Kapsiki Plateau; [19]). The distribution of the spinel compositions in Cr-Al-Fe^{3+} ternary diagram (**Figure 5**) both for Adamawa Plateau and the Cameroon Volcanic Line reflects the heterogeneous nature of the magmatic source. The Ti (0.44 - 0.52 a.p.f.u) and Fe^{2+} (3.15 - 3.59 a.p.f.u) contents are high and could be link to the re-equilibration during the crystallization of the clinopyroxene from the host basalt.

4.2.5. Plagioclase

The compositions of plagioclase (**Table 5**) from the host basalt range from bytownite ($An_{71}Ab_{28}$) to labradorite ($An_{61\text{-}69}Ab_{37\text{-}30}$).

5. Discussion

5.1. Origin of Wehrlites

Ultramafic xenoliths are considered as fragments of lithospheric mantle [1] or the residues of the partial melting of mantle [20].

Clinopyroxenes in the studied wehrlites are low in TiO_2 (0.8 - 1.7 wt%) and Al_2O_3 (1.8 - 5.1 wt% 3 - 4 wt%) as typical for clinopyroxenes of residual mantle origin [14] [13]. The refractory elements as Cr are enriched in the residue, as

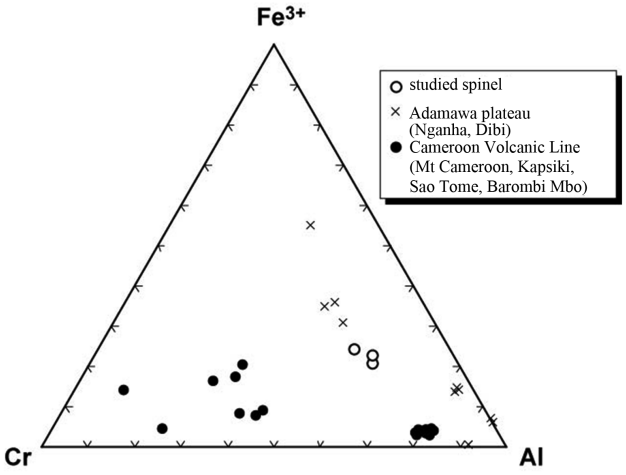

Figure 5. Fe^{3+}-Cr-Al ternary diagram of the spinel for xenoliths from the SW of the Hosséré Dammougalré and those of the others sector of the Adamawa Plateau and the Cameroon Volcanic Line.

Table 3. Representative compositions of Fe-Ti oxides of host basalt.

sample nb.	132	132	132	132	132	132	132
SiO_2 (wt%)	0.00	0.00	0.05	0.03	0.13	1.01	0.07
TiO_2	24.63	24.66	25.03	24.56	19.60	19.59	17.83
Al_2O_3	2.64	2.85	2.35	2.02	2.41	1.51	5.68
Cr_2O_3	0.07	0.21	0.11	0.17	0.50	0.05	0.00
FeO	65.52	63.68	65.83	65.83	67.46	69.58	67.68
MnO	0.74	0.83	0.74	0.86	0.76	2.33	0.64
MgO	3.93	4.51	3.57	3.28	4.02	1.43	4.13
CaO	0.24	0.09	0.06	0.13	0.11	0.22	0.00
Total	97.77	96.84	97.72	96.87	95.18	96.08	96.19
Ilmenite basis							
Fe_2O_3 (calc.)	36.69	35.85	36.11	36.37	41.49	40.88	41.21
FeO (calc.)	32.51	31.42	33.34	33.11	30.13	32.80	29.60
Total (calc.)	101.44	100.43	101.34	100.51	99.14	99.82	99.16
Ulvospinel basis							
Fe_2O_3 (calc.)	20.27	19.41	19.39	19.98	28.31	26.93	29.93
FeO (calc.)	47.28	46.21	48.38	47.86	41.98	45.35	39.75
Total (calc.)	99.80	98.78	99.67	98.87	97.82	98.42	98.03
Si (apfu)	0.000	0.001	0.014	0.008	0.037	0.303	0.021
Ti	5.343	5.374	5.457	5.418	4.346	4.400	3.704
Al	0.898	0.973	0.803	0.698	0.836	0.531	1.960
Cr	0.017	0.049	0.025	0.039	0.117	0.011	0.000
Fe^{3+}	4.399	4.231	4.231	4.411	6.281	6.051	6.591
Fe^{2+}	11.402	11.194	11.729	11.739	10.350	11.327	9.728
Mn	0.180	0.204	0.180	0.212	0.190	0.590	0.159
Mg	1.689	1.947	1.542	1.434	1.766	0.638	1.800
Ca	0.073	0.028	0.020	0.041	0.034	0.069	0.000
Usp (%)	68.09	68.64	69.59	68.89	55.90	59.46	48.54

Table 4. Representative compositions of the spinel of the studied wehrlite.

sample nb.	132-1	132-1	132-1
TiO_2 (wt%)	2.92	2.48	2.85
Al_2O_3	32.62	32.64	28.78
Cr_2O_3	14.90	14.26	16.15
FeO	33.62	35.77	39.57
MnO	0.32	0.23	0.50
MgO	14.11	13.65	10.84
CaO	0.01	0.00	0.06
Total	98.73	99.04	98.74
Fe_2O_3 (calc)	17.82	19.36	19.58
FeO (calc)	17.58	18.34	21.95
Total (calc)	100.52	100.98	100.7
Ti (apfu)	0.516	0.439	0.522
Al	9.042	9.044	8.259
Cr	2.771	2.651	3.109
Fe^{3+}	3.154	3.426	3.588
Fe^{2+}	3.458	3.607	4.471
Mn	0.063	0.046	0.102
Mg	4.949	4.786	3.934
Ca	0.003	0.000	0.015

Table 5. Representative compositions of the plagioclase of the host basalt.

sample nb.	132	132	132	132	132	132
SiO_2 (wt%)	50.71	50.67	52.08	49.4	50.63	51.66
Al_2O_3	28.40	30.51	30.31	32.34	30.66	31.25
FeO	1.30	0.70	0.55	0.39	0.54	0.68
CaO	12.93	12.4	12.07	14.11	13.55	13.86
Na_2O	4.12	3.84	4.13	3.20	3.25	3.30
K_2O	0.66	0.34	0.34	0.15	0.25	0.24
Total	98.12	98.46	99.48	99.57	98.88	100.98
Si (apfu)	2.319	2.335	2.371	2.26	2.331	2.331
Al	1.531	1.657	1.626	1.744	1.664	1.661
Fe^{2+}	0.000	0.027	0.021	0.015	0.021	0.026
Ca	0.634	0.612	0.589	0.691	0.668	0.670
Na	0.366	0.344	0.366	0.284	0.291	0.289
K	0.038	0.020	0.02	0.009	0.015	0.014
An (%)	64	64	61	71	69	69
Ab	32	34	37	28	30	30
Or	3	2	2	1	2	1

demonstrated for the Cr-rich clinopyroxene from the studied xenoliths. Thus, the studied spinel-bearing wehrlite xenoliths, characterized by the presence of Cr-diopside, represent probably the residual portions of the upper mantle [21]. The range of Ni contents (up to 1900 ppm) of olivine of wehrlites from the SW of Hosséré Dammougalré confirms that they are residues of melting. However, the compositions of olivine crystals which are characterized by the forsterite contents lower than 90%, may, have been modified by Fe-Mg equilibration between wehrlite olivine and the host basalt. Re-equilibration between Fe-Mg and host basalt at low temperatures is corroborated by slight similarity between wehrlite olivine Mg# (Fo76 - 88), NiO (0.04 - 0.19 wt.) and CaO (0.15 - 0.39) contents and olivine in host basalt Mg# (Fo68 - 74), NiO (0.04 - 0.16 wt%) and CaO (0.30 - 0.43). Thus, the occurrence of small plagioclase and oxides crystal surrounding the wehrlites indicates that olivine re-equilibration took place at low pressures (<0.2 GPa; [22]).

5.2. Geothermometry and Geobarometry

Equilibrium temperatures calculated from Fe/Mg exchange reaction for olivine/spinel using geothermometers [23] vary between 944˚C and 1102˚C. These temperatures are near of that estimated at liquidus above 1150˚ C after [24] for the crystallization of the Cr-spinel.

The CaO contents (0.15 - 0.39 wt%) of the studied wehrlite olivine are obviously higher than that of olivine of mantle origin (0.05% - 0.1%: [17]), which involve low pressure (<0.2 GPa; [22]) equilibrium environment, probably near the surface. However, as evidenced by the Al^{vi} *vs* Al^{iv} diagram (see **Figure 6**) all the analyzed wehrlite clinopyroxenes have crystalized at high pressures [13] near of the RMC (Refractory Mantle Clinopyroxene; [14]) field. These contrasted results, would indicate that the wehrlite clinopyroxene would have been re-equilibrated in the host basalt at high pressures (shallow depths) during their as

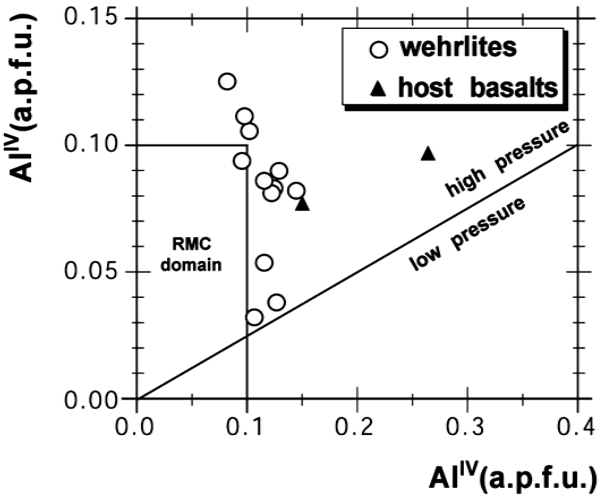

Figure 6. Al^{VI} vs. Al^{IV} (apfu) plot of clinopyroxene from ultramafic xenoliths and host basalt. Field for refractory mantle clinopyroxenes (RMC) after Jagoutz *et al.* (1979).

cending towards the surface. As estimated for Ngao Voglar xenoliths [5], which are situated in the same geological domain (Adamawa Plateau), the wehrlite xenoliths from the SW of Hosséré Dammougalré have likely been entrained by host basalt and carried up to the earth's surface from the depth limit of 57 - 58 km.

6. Conclusion

Petrographical, mineral chemistry and thermobarometric data indicated that the wehrlite xenoliths from the SW of Hosséré Dammougalré are likely residual portions of the mantle partial melting, strongly re-equilibrated by the host melt which were extracted from shallow depths (~60 km) at temperatures estimated around 1100˚C.

Acknowledgements

The French "Ministère de la Coopération" is acknowledged for providing a grants to I.B.G.M. for nine-month stay in France at the "Laboratoire de magmatologie et de géochimie inorganique et expérimentale, Université Pierre-et-Marie-Curie", Paris. Pr Bernard Déruelle is acknowledged for his assistance and his supervision during the laboratory-work at this university.

References

[1] Menzies, M., Rodgers, N., Tindle, A. and Hawkesworth, C. (1987) Metasomatic and Enrichment Processes in Lithospheric Peridotites, an Effect of the Asthenosphere-Lithosphere Interaction. In: Menzies, M. and Hawkesworth, C.J., Eds., Mantle Metasomatism Academic Press, London, 313-361.

[2] Girod, M., Dautria, J.-M., Ball, E. and Soba, D. (1984) Estimation of the Depth of Moho under the Volcanic Massif of Adamaoua (Cameroon), from the Study of Enclaves of Lherzolite. *Comptes Rendus de l'Académie des Sciences Paris, Série II*, **298**, 699-704.

[3] Dautria, J.-M. and Girod, M. (1986) The Enclaves of the Spinel and Plagioclase Lherzolite of the Dibi Volcano (Adamaoua, Cameroon): Witnesses of an Abnormal upper Mantle. *Bulletin de Minéralogie*, **109**, 275-286.

[4] Temdjim, R. (2005) Contribution to the Knowledge of the upper Mantle of Cameroon through the Study of the Ultrabasic and Basic Enclaves by the Volcanoes of Youkou (Adamaoua) and Nyos (Cameruon Line). Thèse de Doctorat d'Etat, Université de Yaoundé I, Yaounde, 339.

[5] Nkouandou, O.F. and Temdjim, R. (2011) Petrology of Spinel Lherzolite Xenoliths and Host Basaltic Lava from Ngao Voglar Volcano, Adamawa Massif (Cameroon Volcanic Line, West Africa): Equilibrium Conditions and Mantle Characteristics. *Journal of Geoscience*, **56**, 375-387.

[6] Nguihdama, D., Chazot, G., Kamgang, P., Mbowou. G.I.B. and Ngounouno, I. (2014) Spinel-Bearing Lherzolite Xenoliths from Hosséré Garba (Likok, Adamawa-Cameroon): Mineral Compositions and Geothermobarometric Implications. *International Journal of Geosciences*, **5**, 1435-1444. https://doi.org/10.4236/ijg.2014.512117

[7] Moreau, C., Regnoult, J.-M., Déruelle, B. and Robineau, B. (1987) A New Tectonic

Model for the Cameroon Line, Central Africa. *Tectonophysics*, **139**, 317-334. https://doi.org/10.1016/0040-1951(87)90206-X

[8] Cornacchia, M. and Dars, R. (1983) Un trait structural majeur du continent africain: les linéaments centrafricains du Cameroun au golfe d'Aden [A Major Structural Feature of the African Continent: The Cameroonian Lineaments to the Gulf of Aden]. *Bulletin de la Société Géologique de France*, **25**, 101-109. https://doi.org/10.2113/gssgfbull.S7-XXV.1.101

[9] Pouchou, J.L. and Pichoir, F. (1991) Quantitative Analysis of Homogeneous or Stratified Microvolumes Applying the Model "PAP". In: Heinrich, K.F.J. and Newbury, D.E., Eds., *Electron Probe Quantification*, Plenum Press, New York, 31-75. https://doi.org/10.1007/978-1-4899-2617-3_4

[10] Roeder, P.L. and Emslie, R.F. (1970) Olivine-Liquid Equilibrium. *Contributions to Mineralogy and Petrology*, **29**, 275-289. https://doi.org/10.1007/BF00371276

[11] Ngounouno, I. and Déruelle, B. (2007) Petrology of Wehrlites and Clinopyroxenites Xenoliths from Mount Cameroon: Evidence of Mantle Metasomatism. *Journal of Cameroon Academy of Science*, **7**, 35-46.

[12] Morimoto, N. (1989) Nomenclature of Pyroxenes. *Canadian Mineralogist*, **27**, 143-156. https://doi.org/10.2465/minerj.14.198

[13] Wass, S.Y. (1979) Multiple Origins of Clinopyroxenes in Alkali Basaltic Rocks. *Lithos*, **12**, 115-132.

[14] Jagoutz, E., Palme, H., Baddenhausen, H., Blum, K., Cendales, M., Dreibus, G., Spettel, B., Lorenz, V. and Wänke, H. (1979) The Abundances of Major, Minor, and Trace Elements in the Earth's Mantle as Derived from Primitive Ultramafic Nodules. *Procedures Lunar Science Conference*, **10**, 2031-2050.

[15] Nono, A., Déruelle, B., Demaiffe, D. and Kambou, R. (1994) Tchabal Nganha Volcano in Adamawa (Cameroon): Petrology of a Continental Alkaline Lava Series. *Journal of Volcanology and Geothermal Research*, **60**, 147-178.

[16] Caldeira, R. and Munhá, J.M. (2002) Petrology of Ultramafic Xenoliths from São Tomé Island, Cameroon Volcanic Line (Oceanic Sector). *Journal of African Earth Science*, **34**, 231-246.

[17] Lee, D.-C., Halliday, A.N., Davies, G.R., Essene, E.J., Fitton, J.G. and Temdjim, R. (1996) Melt Enrichment of Shallow Depleted Mantle: A Detailed Petrological, Trace Element and Isotopic Study of Mantle-Derived Xenoliths and Megacrysts from the Cameroon Line. *Journal of Petrology*, **37**, 415-441. https://doi.org/10.1093/petrology/37.2.415

[18] Wandji, P., Tsafack, J.P.F., Bardintzeff, J.M., Nkouathio, D.G., Kagou Dongmo, A., Bellon, H. and Guillou, H. (2009) Xenoliths of Dunites, Wehrlites and Clinopyroxenite in the Basanites from Batoke Volcanic Cone (Mount Cameroon, Central Africa): Petrogenetic Implications. *Mineralogy and Petrology*, **96**, 81-98. https://doi.org/10.1007/s00710-008-0040-3

[19] Ngounouno, I., Dagwaï, N., Kamgang, P. and Deruelle, B. (2008) Petrology of Spinel Lherzolite Xenoliths in Alkali Basalts from Liri, South of the Kapsiki Plateau (Northernmost Cameroon Hot Line). *Journal of Cameroon Academy of Science*, **8**, 31-42.

[20] Frey, F.A. and Prinz, M. (1978) Ultramafic Inclusions from San Carlos, Arizona: Petrological and Geochemical Data Bearing on Their Petrogenesis. *Earth and Planetary Science Letters*, **38**, 129-176.

[21] Mysen, B.O. and Kushiro, I. (1977) Compositional Variations of Coexisting Phases

with Degrees of Melting of Peridotite in the Upper Mantle. *American Mineralogist*, **62**, 843-865.

[22] Brey, G.P. and Kohler, T. (1990) Geothermobarometry in Four-Phase Lherzolites II, New Thermobarometers, and Practical Assessment of Existing Their Barometers. *Journal of Petrology*, **31**, 1353-1378. https://doi.org/10.1093/petrology/31.6.1353

[23] Roeder, L.P., Campbell, I.H. and Jameson, H.E. (1979) A Re-Evaluation of the Olivine-Spinel Geothermometer. *Contributions to Mineralogy and Petrology*, **68**, 325-334. https://doi.org/10.1007/BF00371554

[24] Thy, P. (1983) Spinel Minerals in Transitional and Alkali Basaltic Glasses from Iceland. *Contributions to Mineralogy and Petrology*, **83**, 141-149. https://doi.org/10.1007/BF00373087